Available online at www.sciencedirect.com
ScienceDirect
Journal of Food Engineering 81 (2007) 741–749
JOURNAL OF FOOD ENGINEERING
www.elsevier.com/locate/jfoodeng

Gabor feature-based apple quality inspection using kernel principal component analysis

Bin Zhu [a], Lu Jiang [a], Yaguang Luo [b], Yang Tao [a,*]

[a] *Bioimaging and Machine Vision Laboratory, Fischell Department of Bioengineering, University of Maryland, College Park, MD 20742, United States*
[b] *Produce Quality and Safety Laboratory USDA ARS, 10300 Baltimore Avenue, Bldg. 002, Rm 117, Beltsville, MD 20705, United States*

Received 13 November 2006; received in revised form 9 January 2007; accepted 9 January 2007
Available online 27 January 2007

Abstract

Automated inspection of apple quality involves computer recognition of good apples and blemished apples based on geometric or statistical features derived from apple images. This paper introduces a Gabor feature-based kernel principal component analysis (PCA) method by combining Gabor wavelet representation of apple images and the kernel PCA method for apple quality inspection using near-infrared (NIR) imaging. First, Gabor wavelet decomposition of whole apple NIR images was employed to extract appropriate Gabor features. Then, the kernel PCA method with polynomial kernels was applied in the Gabor feature space to handle non-linear separable features. The results show the effectiveness of the Gabor-based kernel PCA method in terms of its absolute performance and comparative performance compared to the PCA, kernel PCA with polynomial kernels, Gabor-based PCA and the support vector machine methods. Using the proposed Gabor kernel PCA eliminated the need for local feature segmentation, but also resolved the non-linear separable problem. An overall 90.6% recognition rate was achieved.

Keywords: Gabor wavelet; Principal component analysis (PCA); Kernel PCA; Gabor-based kernel PCA; Apple quality inspection; Near-infrared

1. Introduction

As one of the most widely used imaging technologies, automated machine vision has recently received more attention in the automated sorting and quality inspections of apples. The rapid development in this area can be seen in both hardware and software advances. On the hardware side, researchers have investigated almost all of the light spectra, from short to long wavelengths, and embedded them into different imaging devices for automated apple sorting and grading (Brown, Segerlind, & Summit, 1974; Leemans, Magein, & Destain, 1999; Shahin, Tollner, McClendon, & Arabnia, 2002; Yang & Marchant, 1996). Furthermore, non-optical hardware-based approaches, such as MRI imaging (Zion, Chen, & McCarthy, 1995), as well as multi-modality imaging (Ariana, Guyer, & Shrestha, 2006; Throop, Aneshansley, & Anger, 1999; Wen & Tao, 1998; Wen & Tao, 2000) and hyperspectral imaging (Lu, 2003) techniques have also been explored by investigators to seek better automated apple processing. Detailed reviews about hardware development have been created (Zhu, Jiang, Cheng, & Tao, 2005; Zhu, Jiang, & Tao, 2007). On the software side, tremendous computer-based pattern recognition approaches have been employed or developed for automated apple sorting applications.

Software advances include Leemans et al. (1999) who applied a Bayesian classifier to segment defects of Jonagold apples based on the color images of bi-color apples. The Bayesian classifier worked well for most Jonagold apple defects; however, misclassification happened between russet and the transition area from ground to blush color. Leemans, Magein, and Destain (2002) proposed a six-step process for grading Golden Delicious and Jonagold apples. The proposed method achieved the classification rates of 78% and 72%, for Golden

* Corresponding author. Tel.: +1 301 405 1189.
E-mail address: ytao@umd.edu (Y. Tao).

0260-8774/$ - see front matter © 2007 Elsevier Ltd. All rights reserved.
doi:10.1016/j.jfoodeng.2007.01.008

Delicious and Jonagold apples, respectively. However, identifying the apple stem-end and calyx from defects was still a problem because the stem-end/calyx often exhibited similar patterns as the apple defects, such as image intensity and 2D size. Yang and Marchant (1996) employed a flooding algorithm to coarsely segment out apple defects, followed by an active contour model to refine the segmentation so that the localization and size accuracy of the detected blemishes could be improved. However, the parameters used in the active contour model varied with different kinds of apples as well as the defects, making it difficult to choose a general set of parameters for the active contour model. In addition, stem-ends and calyx could be misclassified as defects when the stem-ends and/or calyx were in view of acquisition cameras. Zion et al. (1995) developed a fast computerized method to detect bruises from MRI images of apples. A simple thresholding technique was used and combined with apple geometry information to distinguish between the apple vascular system and bruises. Although, the internal 3D structure of an apple could be obtained with MRI imaging technology, the cost of both computation time and the system itself was very high. Nakano (1997) employed two neural networks to color grade Sun Fuji apples. A three-layered neural network with seven input nodes and six output nodes was used to evaluate whether the color of the apple surface was normal red or abnormal red with an overall accuracy about 95%. Another three-layered neural network with eleven input nodes and five output nodes was applied to grade the color of apples into five quality categories with an overall 70% recognition rate. However, the recognition rate for some quality classes was very low (<40%). Wen and Tao (1999) built a rule-based machine vision system to detect apple defects. A binary decision-tree-structured rule base was established by blob feature analysis. Although, a relatively high recognition rate for good and defective apples could be achieved by choosing appropriate parameters, the misclassification between stem-end/calyx and defects still existed. Unay and Gosselin (2003) used principal component analysis (PCA) for quality grading of Jonagold apples. The performance of both direct PCA and separate PCA was compared and discussed, and the separate PCA showed a higher recognition rate. Unay and Gosselin (2005) later applied an artificial neural network (ANN) to segment apple defects by pixel-wise processing. They also tested and compared five supervised classifiers, and the results showed that the adaboost and support vector machine (SVM) were the best two classifiers with above 90% recognition rates. Cheng et al. (2004) proposed an integrated PCA-FLD (Fisher linear discriminant) method to maximize the representation and classification effects on the extracted feature bands of high-resolution hyperspectral images. An overall recognition rate of 93% was achieved. However, the testing features need to be segmented manually, which makes this approach currently unavailable for the automated industry application.

Although, pattern recognition techniques are widely used in automated apple quality inspections, most approaches are based on local information and need local feature segmentation. However, local feature extraction itself remains a very challenging problem in image processing. Global feature based techniques, however, can be found in many other pattern analysis and computer vision fields (e.g., whole facial image based human face recognition (Turk & Pentland, 1991)).

The objective of this research was to introduce a global feature-based approach that would eliminate the need for image segmentation, and hence became a feasible method for automated high-speed industrial applications. A Gabor-based kernel PCA method (Liu, 2004; Shen & Bai, 2004), which combined Gabor wavelet representation of the apple features and the kernel PCA, was used for apple quality inspection based on NIR images. In this paper, Gabor wavelet decomposition is introduced in Section 2.2. In Section 2.3, kernel PCA and Gabor-based kernel PCA are demonstrated in details. For comparison purposes, SVM is introduced in Section 2.4. The experimental results and comparisons to five different classification schemes are given in Section 3 to show the effectiveness of the Gabor-based kernel PCA approach for apple quality inspection.

2. Materials and methods

2.1. System and dataset

The machine vision system (Fig. 1a) for apple quality inspection consists of a computer-controlled image grabbing module and a NIR sensing system, which is a monochromatic CCD camera (Hitachi KP-MI) with a C-mount lens of 16 mm focal length and a 700 nm long-pass interference filter (Corrion). The NIR images are grabbed and analyzed by a host computer equipped with a Matrix Meteor/RGB imaging board. A lighting chamber was designed to provide uniform illumination for the infrared sensor (Cheng, Tao, & Chen, 2003). The $120(W) \times 100(L) \times 25(H)\,\mathrm{cm}^3$ chamber is made of lattice-patterned sheet metal, and the v-shaped interior surface of the chamber is painted flat white to provide diffuse light reflection and eliminate shadows (Tao, Chance, & Liu, 1995). In order to provide lighting, ten warm-white fluorescent lamps are mounted uniformly around a v-shaped surface right above the conveyor. The NIR imaging sensor is mounted inside on the top center of the chamber. A roller conveyor belt is built to hold and move apples in up to six lanes. All apple samples are manually placed on the conveyer belt with a random orientation. The apples are rotating and moving when they pass through the field of view of the NIR camera. The whole surface of each apple can be covered by the NIR camera during the apple rotation. A drive controller and speed controller are connected with an optical encoder that provides precise timing signals for both on-line mechanical and electrical synchronization (Cheng, 2004).

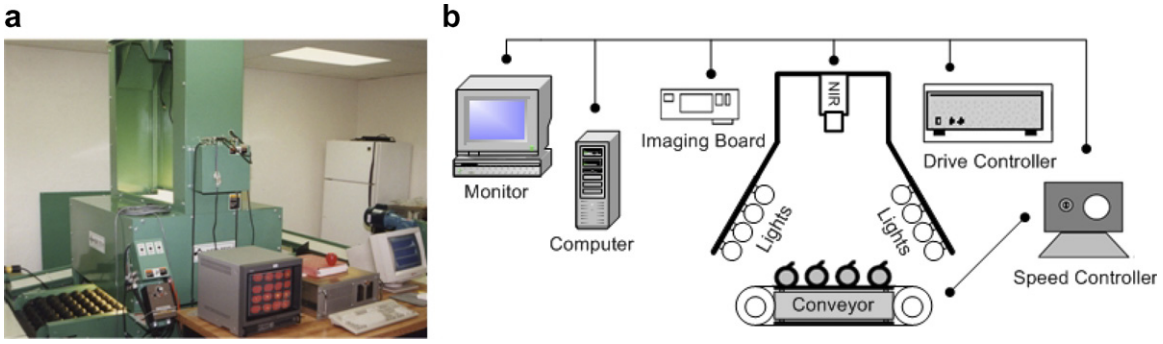

Fig. 1. NIR machine vision system for apple quality inspection. (a) A snapshot of the system. (b) A schematic representation of the system.

The schematic of the whole imaging system is shown in Fig. 1b.

The dataset grabbed by the imaging system contains a total of 166 NIR Golden Delicious apple images, including ones with and without defects. Apples were refrigerated and stored at 4 °C before they were tested. Typical NIR apple images are shown in Fig. 2.

2.2. Gabor-wavelet decomposition

Gabor wavelets have successfully modeled the response of brain cells in the visual cortex (Jones & Palmer, 1987) since they optimally represent the textural structure with different locations and orientations. Gabor-based wavelets (Lades et al., 1993) come from a self-similar family generated from the mother wavelet under groups of translation, rotation and scaling transformations. It has the following general form:

$$\Psi_{\vec{k}}(\vec{z}) = \frac{\vec{k}^2}{\sigma^2} e^{(-\vec{k}^2\vec{z}^2/2\sigma^2)}[e^{i\vec{k}\vec{z}} - e^{-\sigma^2/2}] \quad (1)$$

where $\vec{z} = (x, y)$ are the spatial coordinates. The two terms $e^{i\vec{k}\vec{z}}$ and $e^{-\sigma^2/2}$ are the oscillation and DC part of Gabor wavelets, respectively. Generally, σ is equal to 2π, and if the parameter σ becomes large enough, the DC term can be ignored (Lades et al., 1993; Liu & Wechsler, 2002). The parameter $\vec{k}$ controls the wavelength and orientation of the wavelets and is given by:

$$\vec{k} = k_{p,q} = k_q e^{i\Phi_p} \quad (2)$$

where $k_q = k_{\max}/f^q$, $\phi_p = \pi p/8$, $k_{\max} = \frac{\pi}{2}$, $f = \sqrt{2}$, and $p \in \{0, \ldots, 7\}$ and $q \in \{0, \ldots, 4\}$ identify eight orientation directions and five space frequencies, respectively. Fig. 3 shows the real part and magnitude of Gabor wavelet kernel under five scalings and eight orientations.

The convolution of an image $I(x, y)$ and Gabor-wavelet $\Psi_{\vec{k}}(x, y)$ can be expressed as

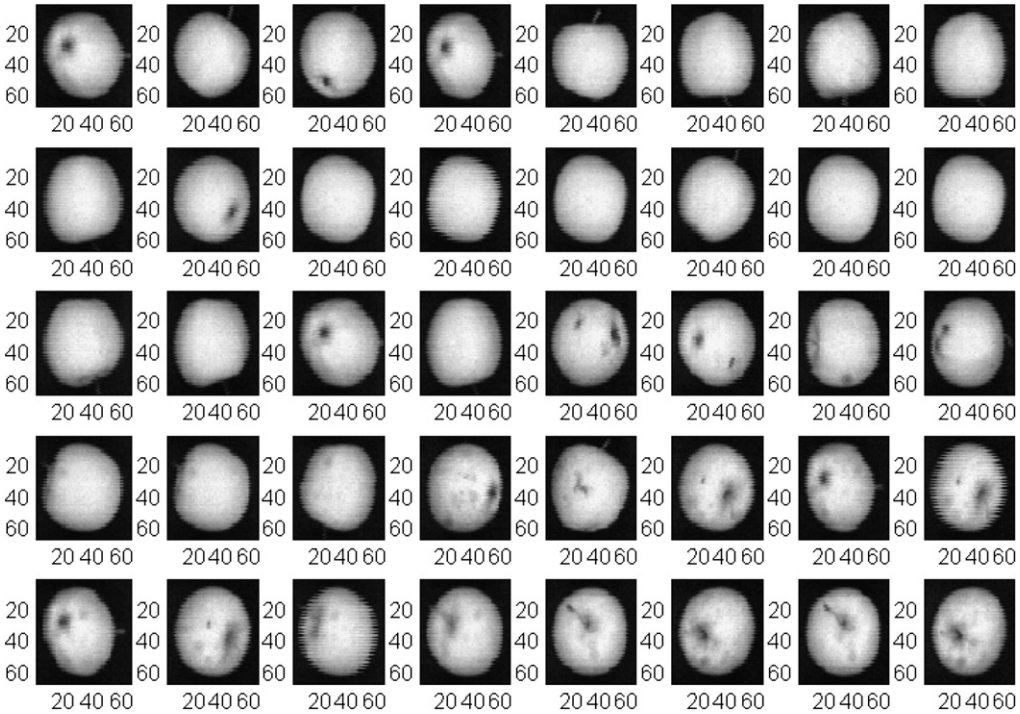

Fig. 2. Example of NIR golden delicious apple image dataset. Numbers surrounding each NIR apple image reflect the actual image size.

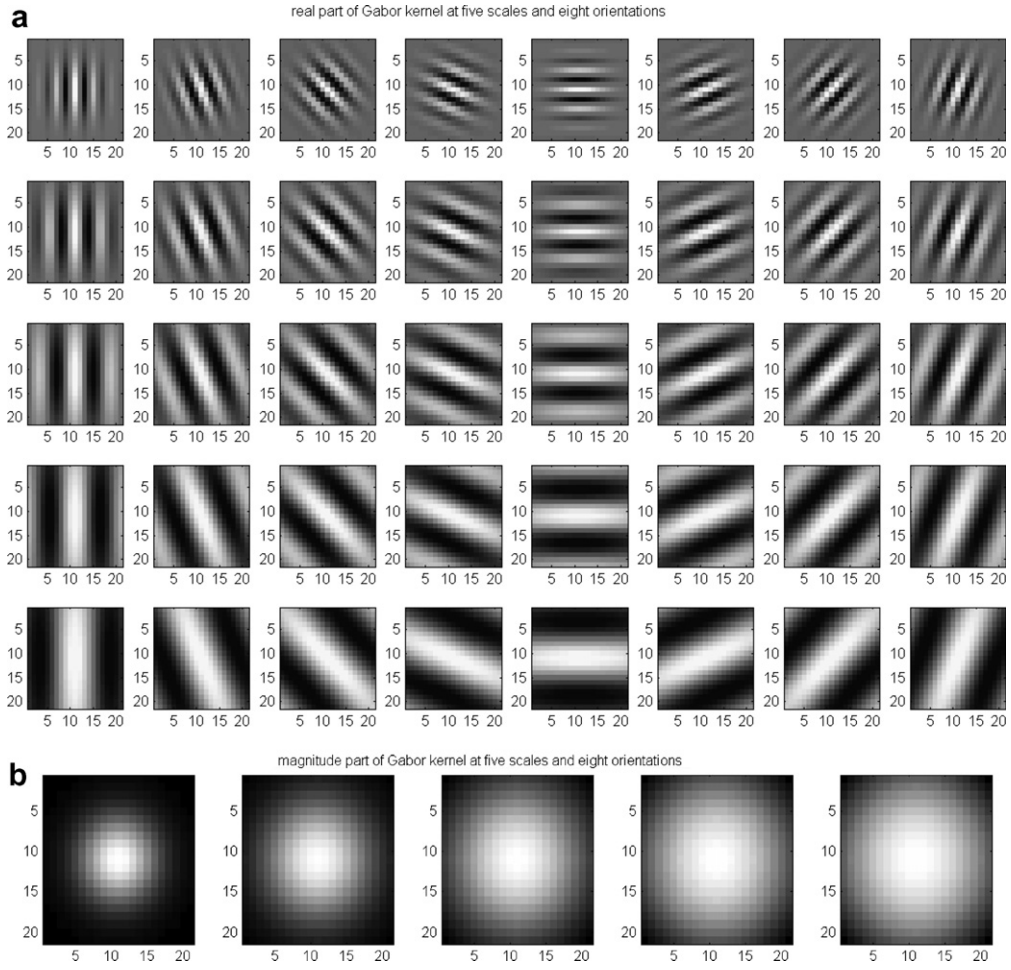

Fig. 3. Gabor wavelet kernels. (a) Real part of Gabor wavelet kernel at 5 scales and 8 orientations. (b) Magnitude part of Gabor wavelet kernel at 5 scales and 8 orientations.

$$F_{\vec{k}}(x,y) = I(x,y) * \Psi_{\vec{k}}(x,y) \tag{3}$$

In the case of eight orientations and five space frequencies, the Gabor feature vector, Ψ, is given by (Liu & Wechsler, 2002):

$$\Psi = (F^t_{0,0} F^t_{0,1} \ldots F^t_{4,7})^t \tag{4}$$

where $F_{p,q}$ is the column vector form of $F_{\vec{k}}$, t is the transpose operator, and Ψ is used as the discriminating features in the apple quality classification.

2.3. Gabor-based kernel PCA

2.3.1. Kernel PCA

PCA (Duda, Hart, & Stork, 2001) has been widely used in many pattern recognition applications, such as face recognition (Belhumeur, Hespanha, & Kriegman, 1997; Turk & Pentland, 1991) and remote sensing (Corner, Narayanan, & Reichenbach, 1999). In this research, PCA was used to define the best subspace such that a set of apple patterns could be sufficiently represented by that subspace. In other words, the goal was to linearly project the input data onto a subspace that maximized the significant variation among the inputs.

Unlike the traditional PCA approach, where only linear projection is performed to seek a best mapping of the original dataset, the kernel PCA (Schölkopf, Smola, & Müller, 1998) relaxes the linear constraint, and allows arbitrary high-order projections among the input data through low-dimensional to high-dimensional mappings. Kernel PCA linearly represents the non-linear problem by means of mapping the low-dimensional input space, which is usually non-linear separable, into a linear separable high-dimensional feature space. More specifically, the underlying principle of kernel PCA is addressed by Cover's theorem (Haykin, 1999). The low- to high-dimensional mapping is defined implicitly by a so-called kernel function, which efficiently computes the inner product as a direct function of the input space. Without explicitly computing the mapping function, the kernel PCA becomes more computationally feasible (Shawe-Taylor & Cristianini, 2004).

Assume the sample set of input space is $\{u_i\}$, $i = 1, \ldots, N$, $u_i \in \Re^n$, and the mean of the sample set is zero. By a non-linear mapping, Φ, the input space can be mapped into another inner product space Γ by

$$\Phi : \Re^n \to \Gamma, \quad u \to U. \tag{5}$$

The dataset in mapped feature space is $\{\Phi(u_1), \Phi(u_2), \Phi(u_3), \ldots. \Phi(u_N)\}$ and the kernel function is defined as the inner product of the data in feature space

$$K(u_i, u_j) = \langle \Phi(u_i), \Phi(u_j) \rangle \tag{6}$$

The kernel matrix, $K \in \Re^{N \times N}$ is

$$K_{ij} = \langle \Phi(u_i), \Phi(u_j) \rangle \tag{7}$$

where $i, j \in \{1, \ldots, N\}$. Schölkopf et al. (1998) proved that the PCA in the inner product feature space could be fulfilled by the equation

$$N\lambda\alpha = K\alpha \tag{8}$$

where K is positive semi-definite kernel matrix, N is the number of samples, λ is the eigenvalue and α is the corresponding eigenvector. Schölkopf et al. (1998) also showed the projection of a test point, $\Phi(u^*)$, onto the eigenvectors V in feature space Γ could be expressed as

$$\langle V, \Phi(u_*) \rangle = \sum_{i=1}^{N} \alpha_i \langle \Phi(u_i), \Phi(u_*) \rangle \tag{9}$$

From Eqs. (7) and (9), the mapped pattern between input space and feature space only needs to be implicitly computed by the inner product.

In general, three kernel functions (Cortes & Vapnik, 1995), which allow computing of the value of the inner product in Γ without carrying out the mapping Φ, are frequently used in kernel classifiers. They are polynomial kernel, Gaussian kernel and sigmoid kernel. The basic idea of kernel PCA is illustrated in Fig. 4 (Schölkopf et al., 1998).

2.3.2. Gabor-based kernel PCA

Gabor-based kernel PCA (Liu, 2004) is combined with the Gabor wavelet decomposition of the sample dataset and kernel PCA for pattern recognition. First, Gabor wavelet decomposition is applied to the sample dataset to obtain the Gabor features of the input data. Then the Gabor feature vector, Ψ is fed into the kernel PCA algorithm. In other words, the Gabor feature space is regarded as the input space of the kernel PCA. Through the kernel PCA, Gabor feature space is mapped to a high-dimensional feature space, Γ, making the high-dimensional features linearly separable by PCA in that space. Finally, the nearest neighbor classifier is used in the high-dimensional space, Γ, to differentiate quality of apples according to the Euclidean distance metric.

2.4. Support vector machine (SVM)

SVM (Duda et al., 2001) is another popular statistical learning algorithm in data mining. It has been widely applied in a large number of applications, such as object recognition (Guo, Li, & Chan, 2000) and face detection (Osuna, Freund, & Girosi, 1997). The key point of this approach is to find the optimal linear hyperplane that can not only properly divide the largest portion of data points, but also maximize the distance of each class from that hyperplane at the same time. Just like the kernel PCA, the input space in SVM can also be mapped into the high-dimensional feature space by kernel function such that the data in the high-dimensional feature space becomes linear separable. However, the classification criterion used in kernel PCA and SVM are different, which makes these two approaches distinctive. For comparison purposes, SVM is also tested in this research. The detection results among different classifiers will be given in the next section.

3. Results and discussion

A total of 166 NIR Golden Delicious apple images were tested in the experiment. Typical Gabor features (5 scalings by 8 orientations) of a NIR apple image are illustrated in Fig. 5. Seen from the Fig. 5, Gabor-wavelet decomposition captures different image information by means of combining different scaling and orientation factors. Given extracted Gabor features, it is important to find an optimal mapping (kernel function) through Gabor feature space to a high dimensional space such that the classification performance in aforementioned high dimensional space can be maximized. For the proposed Gabor-KPCA approach, three typical kernel functions, e.g. Polynomial kernel, Gaussian kernel and Sigmoid kernel, were evaluated in the experiment. The relationship between recognition rate and different kernel functions is plotted in Fig. 6.

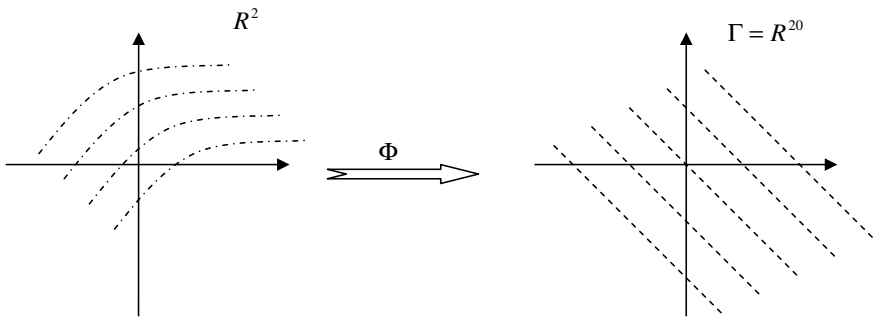

Fig. 4. Illustration of kernel PCA showing non-linearly mapping of the input space (R^2) into the Γ space (R^{20}) with Φ, and then implementing the linear PCA in space Γ.

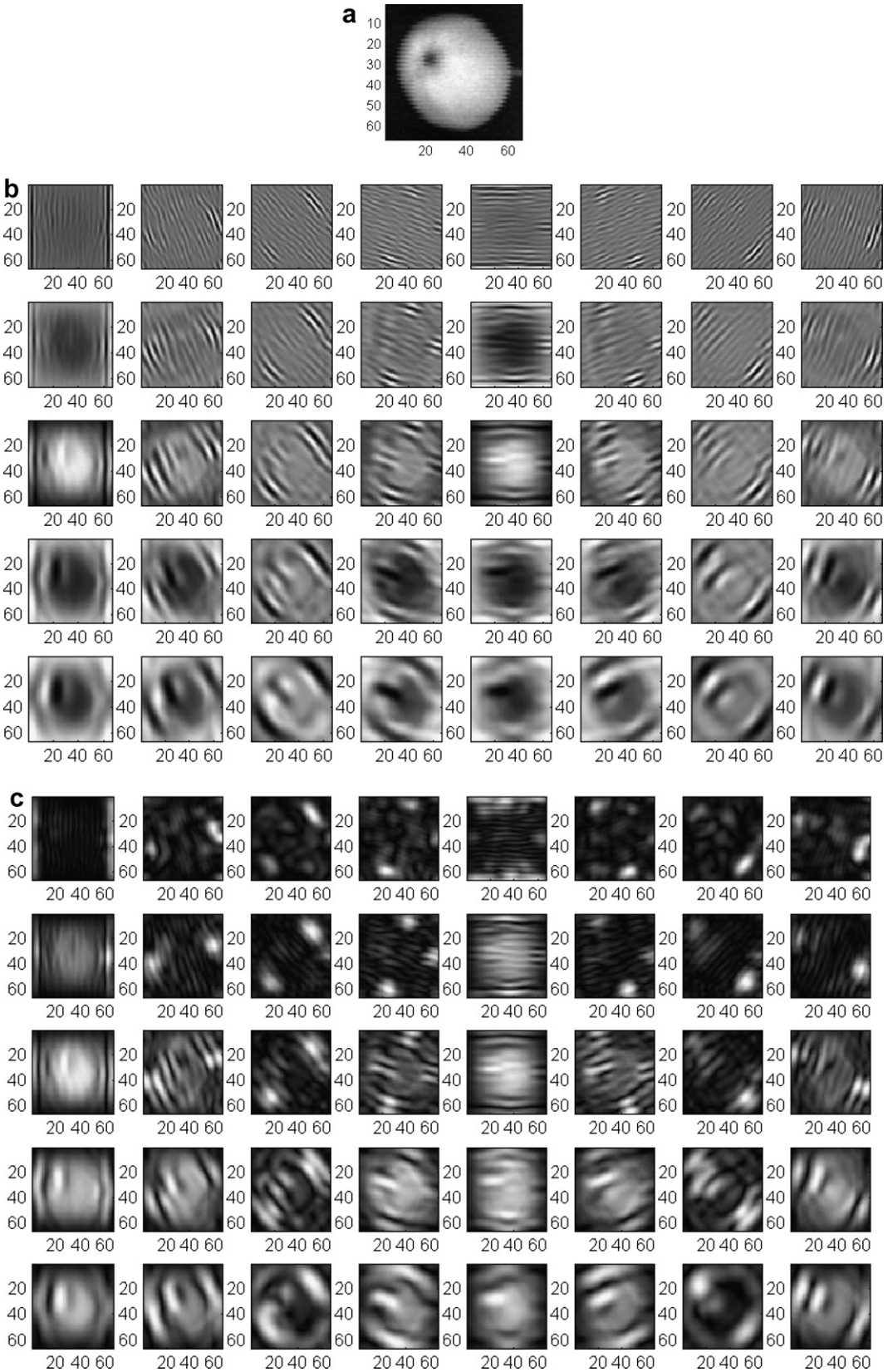

Fig. 5. Gabor wavelet decomposition for a NIR apple image. (a) Original apple NIR image. (b) Real part of Gabor wavelet decomposition. (c) Magnitude of Gabor wavelet decomposition.

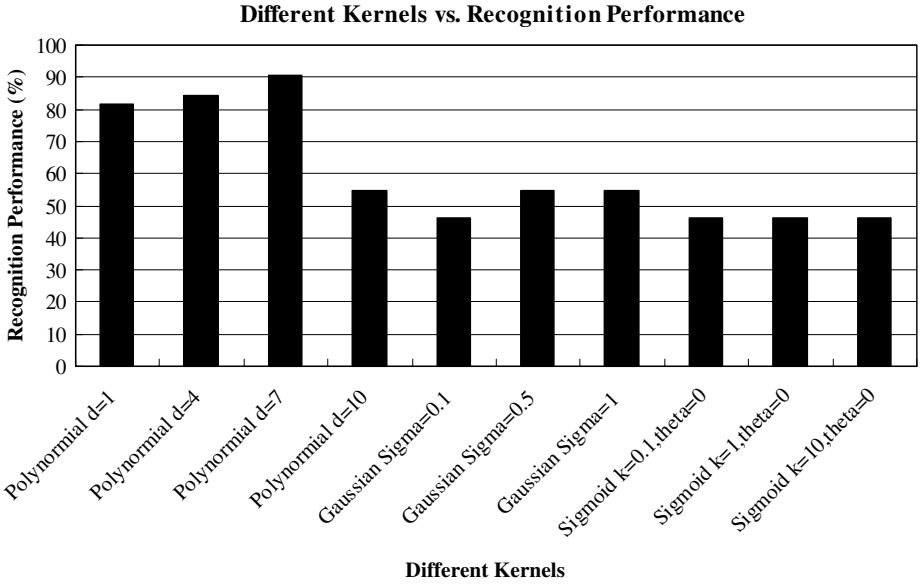

Fig. 6. The relationship between recognition rate and the typical kernel functions with different parameters.

As seen in Fig. 6, the polynomial kernels have the best classification performance among all three kernel types. The recognition rate increases as the degree of freedom increases, and achieves its optimal by 90.5% when degree of freedom equals to 7. The experiment results demonstrate that the high order polynomial mapping from Gabor feature space makes the mapped data more linear separable in the high dimensional space. In other words, the Gabor-KPCA method can linearly solve the non-linear problem through a high order polynomial mapping. As a result, the polynomial kernel with seventh-order was chosen for proposed Gabor-KPCA approach. Table 1 shows the confusion matrix of Gabor-KPCA method.

To further evaluate the proposed Gabor-KPCA approach, the performances of five methods were assessed in the experiment: PCA, Gabor wavelet-based PCA, kernel PCA with polynomial kernels, Gabor based kernel PCA with polynomial kernels, and SVM with polynomial kernels. A total of 40 NIR apple images were used as training samples, and 126 apple images were tested in this research. The dataset was divided into two categories: good or blemished. The recognition rates of each method are given in Table 2. The proposed Gabor-KPCA method had the highest recognition rate comparing to other approaches. Note that the recognition rates of Gabor PCA and kernel PCA were lower than PCA, while the combination of them was higher. This shows that more information can be reserved (meaning better classification performance) through linear representation in original NIR image space rather than in the Gabor feature space. PCA had a higher recognition rate than kernel PCA, illustrating that the non-linear mapping through the polynomial kernel function from original input space (apple NIR image space), not the Gabor feature space, did not make the mapped data more linear separable than the original inputs. This fact can also be found in SVM, since SVM has the same kernel function as kernel PCA. However, when Gabor feature space and the non-linear mapping through the polynomial kernel function are combined together, the recognition performance can be significantly improved. In other words, although Gabor feature space reserves less information under linear representation than original input space, when it is mapped to a high-dimensional space through the polynomial kernel function, the mapped space becomes linear separable.

Table 1
Confusion matrix of proposed Gabor-KPCA method

True labels	Estimated labels		Totals
	Healthy apple	Unhealthy apple	
Healthy apple	50	8	58
Unhealthy apple	4	64	68
Totals	54	72	126

Table 2
Data sets and recognition rates

Approach	Recognition rate (%)
Gabor-kernel PCA	90.5
PCA[a]	84.9
SVM	83.3
Gabor PCA	81.8
Kernel PCA	81.0

[a] *Note*: Although, both recognition rate of individual Gabor PCA and kernel PCA are lower than PCA, the combination of them is higher.

Both types I and II errors (Lyman, 2001) were considered in the study to evaluate the performance of the proposed approach. Type I error is calculated as the number of misclassified samples (i.e. defected apple images) divided by the total number of samples, while type II error is com-

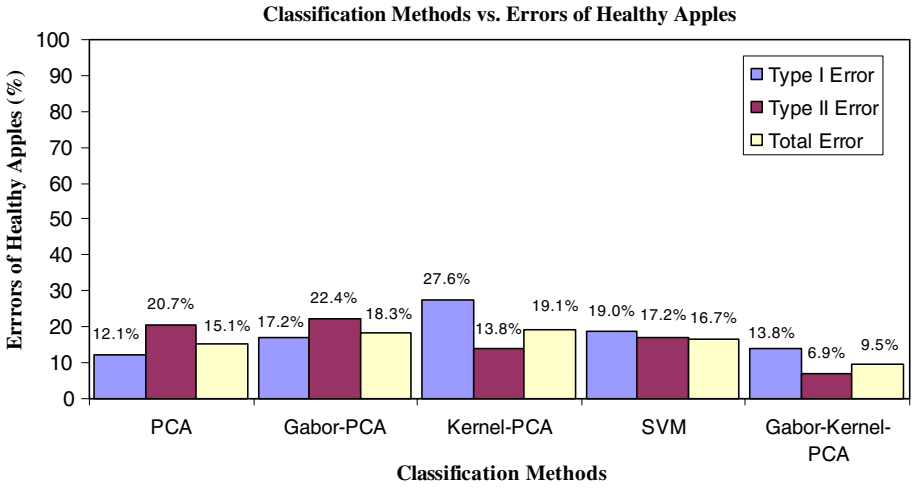

Fig. 7. Error rate for good apples based on five classification approaches.

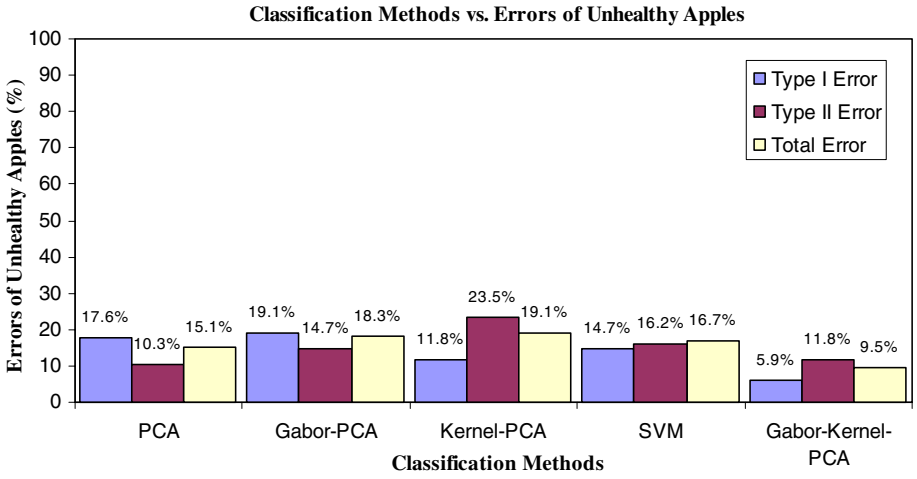

Fig. 8. Error rate for blemished apples based on five classification approaches.

puted as the number of false classified samples over the total number of samples. The error rates for good and blemished apples are given in Figs. 7 and 8, respectively. For good apples, Gabor kernel PCA has the lowest type II error, and second lowest type I error. Although the type I error of the Gabor kernel PCA is slightly higher than PCA, the overall error rate of this approach is still the lowest. Note that PCA has the second highest type II error rate of 20.7%. The same phenomenon can be observed in the damaged apple category. The Gabor kernel PCA has the lowest type I error and second lowest type II error, but it has the best performance in terms of overall error rate. According to the experiment results, the Gabor kernel PCA showed its feasibility to do the apple quality inspection without local feature segmentation.

As a summary, the basic procedure of proposed approach can be illustrated as the following three steps:

(1) Gabor feature extraction using whole apple NIR image.
(2) Data mapping from Gabor feature space to a high-dimensional space through the polynomial kernel function.
(3) Linear representation using PCA and classification using nearest neighborhood approach.

4. Conclusions

This paper introduced a Gabor feature-based kernel PCA approach to inspect the quality of apples. This approach showed many advantages. First, it eliminated the need of local feature segmentation by means of Gabor feature decomposition for the whole apple NIR images. It also sought a better high-dimensional space through the polynomial kernel function, which mapped Gabor feature space to high-dimensional space, and made the non-linear separable problem in the Gabor feature space linear separable in that high-dimensional space. The comparison among five different classifiers was also conducted to eval-

uate the performance of those classifiers, and the experimental results showed that the proposed Gabor kernel PCA had the highest recognition rate among the five classifiers. Based on 166 NIR Golden Delicious apple images, an overall 90.6% detection rate was achieved with this method. In the future, additional data may be acquired to assess the robustness of the proposed approach. More global-based features may need to be explored to improve the performance of automated apple quality inspection. Furthermore, based on various quality conditions and defect types, more class categories may need to be considered to better fit apple industry requirements.

Acknowledgements

Authors thank Dr. Xuemei Chen for helping to set up the imaging system. Thanks also go to Ms. Abby Vogel for her help to improve the style of this manuscript.

References

Ariana, D., Guyer, D. E., & Shrestha, B. (2006). Integrating multispectral reflectance and fluorescence imaging for defect detection on apples. *Computers and Electronics in Agriculture, 50*, 148–161.

Belhumeur, P., Hespanha, J., & Kriegman, D. (1997). Eigenfaces vs. fisherfaces: recognition using class specific linear projection. *IEEE Transactions on PAMI, 19*, 711–720.

Brown, G. K., Segerlind, L. J., & Summit, R. (1974). Near-infrared reflectance of bruised apples. *Transactions of ASAE, 17*(1), 17–19.

Cheng, X., (2004). Hyperspectral imaging and pattern recognition technologies for real time fruit safety and quality inspection. Ph.D. Thesis. University of Maryland, College Park.

Cheng, X., Chen, Y., Tao, Y., Wang, C., Kim, M., & Lefcourt, A. (2004). A novel integrated PCA and FLD method on hyperspectral image feature extraction for cucumber chilling damage inspection. *Transactions of ASAE, 47*(4), 1313–1320.

Cheng, X., Tao, Y., & Chen, Y. R. (2003). NIR/MIR dual-sensor machine vision system for on-line apple stem-end/calyx recognition. *Transaction of ASAE, 46*(2), 551–558.

Corner, B., Narayanan,& R., Reichenbach, S., (1999). Principal component analysis of multisensor remote sensing imagery: effects of additive and multiplicative noise. In *Proceedings of the SPIE 44th Annual Meeting*, Denver, Colorado, 3808, pp. 183–191.

Cortes, C., & Vapnik, V. (1995). Support vector networks. *Machine Learning, 20*, 273–297.

Duda, R., Hart, P., & Stork, D. (2001). *Pattern classification* (2nd ed.). Wiley Interscience.

Guo, G., Li, S.Z., Chan, K., (2000). Face recognition by support vector machines. In *Proceedings of the 4th IEEE International Conference on Automatic Face and Gesture Recognition*, Grenoble, France, pp. 196–201.

Haykin, S. (1999). *Neural networks – a comprehensive foundation* (2nd ed.). Prentice Hall.

Jones, J. P., & Palmer, L. A. (1987). An evaluation of the two-dimensional gabor filter model of simple receptive fields in cat striate cortex. *Journal of Neurophysiology, 58*, 1233–1258.

Lades, M., Vorbruggen, J. C., Buhmann, J., Lange, J., von der Malsburg, C., Wurtz, R. P., et al. (1993). Distortion invariant object recognition in the dynamic link architecture. *IEEE Transactions on Computers, 42*(3), 300–311.

Leemans, V., Magein, H., & Destain, M. –F. (1999). Defect segmentation on Jonagold apples using colour vision and a Bayesian classification method. *Computers and Electronics in Agriculture, 23*, 43–53.

Leemans, V., Magein, H., & Destain, M.-F. (2002). On-line fruit grading according to their external quality using machine vision. *Biosystems Engineering, 83*, 397–404.

Liu, C. (2004). Gabor-based kernel PCA with fractional power polynomial models for face recognition. *IEEE Transactions on PAMI, 26*, 572–581.

Liu, C., & Wechsler, H. (2002). Gabor feature based classification using the enhanced fisher linear discriminant model for face recognition. *IEEE Transactions on Image Processing, 11*(4), 467–476.

Lu, R. (2003). Detection of bruises on apples using near-infrared hyperspectral imaging. *Transactions of ASAE, 46*(2), 523–530.

Lyman, O. (2001). *An introduction to statistical methods and data analysis* (5th ed.). Michael Longnecker.

Nakano, K. (1997). Application of neural networks to the color grading of apples. *Computers and Electronics in Agriculture, 18*, 105–116.

Osuna, E., Freund, R., & Girosi, F., (1997). Training support vector machines: an application to face detection. In *Proceedings of the CVPR'97*, Puerto Rico.

Schölkopf, B., Smola, A., & Müller, K. (1998). Non-linear component analysis as a kernel eigenvalue problem. *Neural Computation, 10*, 1299–1319.

Shahin, M. A., Tollner, E. W., McClendon, R. W., & Arabnia, H. R. (2002). Apple classification based on surface bruises using image processing and neural networks. *Transactions of ASAE, 45*(5), 1619–1627.

Shawe-Taylor, J., & Cristianini, N. (2004). *Kernel methods for pattern analysis*. Cambridge University Press.

Shen, L., & Bai, L., (2004). Gabor feature based face recognition using kernel methods. In *Proceedings of the 6th IEEE International Conference on Automatic Face and Gesture Recognition*, Seoul, Korea, pp. 170–176.

Tao, Y., Chance, L., & Liu, B. (1995). *Full-scale fruit vision sorting system design –factors and considerations. In food processing automation IV*. ASAE Publication, ISBN 0-929355-70-9.

Throop, J.A., Aneshansley, & D.J., Anger, B., (1999). Multispectral images for detecting defects on apples in real time. ASAE Paper No.993205. St. Joseph, Mich.: ASAE.

Turk, M., & Pentland, A. (1991). Eigenfaces for recognition. *Journal of Cognitive Neuroscience, 3*, 72–86.

Unay, D., & Gosselin, B., (2003). A study on quality grading of Jonagold apples. In *Proceedings of the 3rd IEEE International Symposium on Signal Processing and Information Technology*, (IEEE ISSPIT 2003), Germany.

Unay, D., & Gosselin, B., (2005). Artificial neural network-based segmentation and apple grading by machine vision. In *Proceedings of the IEEE ICIP 2005*, Italy.

Wen, Z., & Tao, Y. (1998). Fuzzy-based determination of model and parameters of dual-wavelength vision system for on-line apple sorting. *Optics Engineering, 37*(1), 293–299.

Wen, Z., & Tao, Y. (1999). Building a rule-based machine-vision system for defect inspection on apple sorting and packing lines. *Expert Systems Application, 16*, 307–313.

Wen, Z., & Tao, Y. (2000). Dual-camera NIR/MIR imaging for stem-end/calyx identification in apple defect sorting. *Transaction of ASAE, 43*(2), 449–452.

Yang, Q., & Marchant, John A. (1996). Accurate blemish detection with active contour models. *Computers and Electronics in Agriculture, 14*, 77–89.

Zhu, B., Jiang, L., Cheng, X., & Tao, Y. (2005). 3D surface reconstruction of apples from 2D NIR images. *Proceeding SPIE, 6000*, 242–251.

Zhu, B., Jiang, L., & Tao, Y. (2007). 3D shape enhanced transform for automatic apple stem-end/calyx identification. *Optical Engineering, 46*(1), 017201.

Zion, B., Chen, P., & McCarthy, M. J. (1995). Detection of bruises in magnetic resonance images of apples. *Computers and Electronics in Agriculture, 13*, 289–299.